Journal of Minerals and Materials Characterization and Engineering, 2024, 12, 316-333
https://www.scirp.org/journal/jmmce
ISSN Online: 2327-4085
ISSN Print: 2327-4077

Peak Particle Velocity Predicting Equation Associated with the Propagation of Vibrations Induced by Blasting in a Mine and Impacts on the Physical Degradation of Houses: The Case of the Yaramoko Mine, Bagassi, Burkina Faso

Richard Zoundi[1,2], Antoine Béré[1], Joel Martial Balkoulga[1], Philibert Sawadogo[2]

[1]Laboratoire de Physique et de Chimie de l'Environnement (LPCE), Université Joseph KI-ZERBO, Ouagadougou, Burkina Faso
[2]Yaramoko Mine, Roxgold Sanu, Bagassi, Burkina Faso
Email: richard__zoundi@yahoo.fr

How to cite this paper: Zoundi, R., Béré, A., Balkoulga, J.M. and Sawadogo, P. (2024) Peak Particle Velocity Predicting Equation Associated with the Propagation of Vibrations Induced by Blasting in a Mine and Impacts on the Physical Degradation of Houses: The Case of the Yaramoko Mine, Bagassi, Burkina Faso. *Journal of Minerals and Materials Characterization and Engineering*, **12**, 316-333.
https://doi.org/10.4236/jmmce.2024.126020

Received: September 7, 2024
Accepted: November 1, 2024
Published: November 4, 2024

Abstract

This study utilizes empirical equations to describe the propagation of vibrations induced by blasting, with the goal of predicting the attenuation of Peak Particle Velocity (PPV) at the Yaramoko mine in Bagassi, Burkina Faso, a site characterized by granitoid rock. Four empirical PPV prediction equations were employed, so-called Duvall & Fogelson (or the United States Bureau of Mines "USBM"), Langefors and Kihlstrom, Ambressys-Hendron, and the Bureau of Indian Standard. The constant parameters for each of these equations, referred to as site constants, were derived from linear regression curves. The results show that the site constants k, a, and b of 4762, 0.869, and 1.737, respectively, derived from the general prediction equation by Davies, PPV = kQ^aD^{-b}, based on Duvall & Fogelson, are in good agreement with values of 4690, 0.9, and 1.69, respectively, for similar rock types in Spain. Regarding the impacts of blasting on houses, the findings indicate that houses built from laterite-block bricks in the village of Bagassi are the most vulnerable to vibration waves, followed by those constructed with cinder-block bricks. In contrast, houses made of banco bricks are the most resilient. Additionally, it was determined that during blasting operations, adjusting the blasting parameters to ensure the PPV does not exceed 2 mm/s at the level of nearby dwellings can minimize the appearance of cracks in houses.

Keywords

Peak Particle Velocity, Blasting, Propagation of Blasting Vibrations, Cracks

on Houses, PPV Equation

1. Introduction

Explosive blasting is commonly practiced at the initial stages of the industrial mining process, particularly when dealing with massive and hard rocks. It is used in all operational mines in Burkina Faso due to the geological context, which is dominated by Birimian crystalline formations [1] (Lower Proterozoic) consisting of schists, quartzites, sandstones, conglomerates, and greenstone rocks. These formations, which cover 80% of the country's territory, are characterized by their high hardness [2].

On mining sites in Burkina Faso, blasting is either conducted by technical personnel or outsourced to specialist companies, such as African Explosives Limited (AEL Burkina), Bulk Mining Explosives, African Underground Mining Services (AUMS), or Maxam Explosives Company. While different types of explosives are used across various sites, they all serve a single purpose: to detach the targeted rock from the massif through the shockwave created by the explosion, which leads to its fragmentation and reduction to smaller grain sizes that can easily be collected by mobile equipment to continue the production process.

As a principle of explosive blasting, an explosion is initiated when a highly flammable chemical compound is compressed into a hole. Detonating such a device generates a significant shockwave that cracks the rock and produces a large volume of gas. This gas, at a very high temperature, diffuses into existing faults or those created by the shockwave, pushing against the rock walls until quasi-static equilibrium is reached. This equilibrium is then broken due to the overpressure caused by the ultra-rapid decomposition of the explosive material. It is this release of energy, exceeding the physical and mechanical strength of the rock mass, that leads to the fragmentation of the rock, which is the primary goal of explosive blasting. Today, explosive blasting is essential in both quarrying and mining due to its many advantages, primarily time and energy savings. Theoretically, a single ton of explosives can fragment approximately 2500 m^3 of rock in less than three seconds. Achieving the same result with a 5-ton hydraulic rock breaker would take 25 days of 10-hour shifts, totaling 250 hours of work [3]. However, there are significant concerns associated with blasting, as the outcomes and impacts remain the focus of considerable attention and can serve as performance indicators for the company. The primary goals of blasting include (i) maximizing the amount of rock fragmented, (ii) achieving the maximum reduction in rock size, and (iii) minimizing the impact of blasting on the surrounding physical and social environment. These objectives must be met under the safest possible conditions, both during the preparation of the blast and during the collection of the fragmented rocks. In terms of the external environment, efforts must be made to prevent rock projections in quarries and open-pit mines, as well as to control noise and vibration

parameters that are considered in the environmental management of projects. Note that in blasting operation, only 20% to 30% of the explosive energy is used for rock breakage and movement, while most of the explosive energy is wasted and not being used effectively. The wasted energy is the main cause of the blasting-induced environmental and sanitary impacts, including fly rock, air blast, and ground vibration, which are undesirable phenomena [4] [5].

It is well established that blasting impacts buildings. **Figure 1** illustrates the physical degradation of the witness houses exposed to blasts at the mine site. As discussed in Section 3.2, the physical degradation of these buildings is the result of the vibration waves generated by the explosive blasts they endure.

It is possible to predict the propagation of vibration waves induced by blasting in a mine by measuring the velocity levels of explosions following blasting and correlating these measured values with field data, such as the explosive charge used and the distance of impact measurement. Understanding the law governing the propagation of vibration waves induced by blasting in a mine allows for determining the explosive charge values that may cause physical damage to buildings and, consequently, helps in limiting such damage. This study is the first to focus on predicting Peak Particle Velocity (PPV) associated with the propagation of vibrations induced by blasting at the Yaramoko mine in Bagassi, Burkina Faso, and can serve as a reference for establishing acceptable values for similar conditions in Burkina Faso.

2. Materials and Methods

2.1. General Information on the Study Area

The study was conducted at Roxgold Sanu, an underground mine that is a subsidiary of Fortuna Mining Corp. This mine is located within the Yaramoko mining permit area in Bagassi, Burkina Faso. Roxgold Sanu is situated near the town of Bagassi in the Balé Province, approximately 200 km southwest of Ouagadougou, the capital of Burkina Faso. A general overview map of the study area is shown in **Figure 2**.

Several zones of gold mineralization are present within the Yaramoko project. The target gold mineralization for this study is located in the 55 Zone, hosted in a narrow, east-northeast-trending shear zone. From 0 to 400 meters (m) in depth, the shear zone dips moderately (65˚ to 70˚) to the south and contains thick extensional quartz veins. Below this depth, the shear zone becomes steeper (85º) with fewer, more segmented, and deformed quartz veins. The bulk of the gold mineralization is found in dilatational segments of the reverse dextral shear zone, where the quartz veins are thicker and exhibit greater geological continuity. Gold typically occurs as coarse free grains in quartz, often associated with minor pyrite. The gold-bearing veins range in width from a few centimeters to over 4 m.

Longhole open stoping (including uphole retreat in certain areas) is the primary mining method, with limited use of cut and fill for crown pillar mining. The mine plan comprises 73% standard long hole stoping with down holes on 17 m

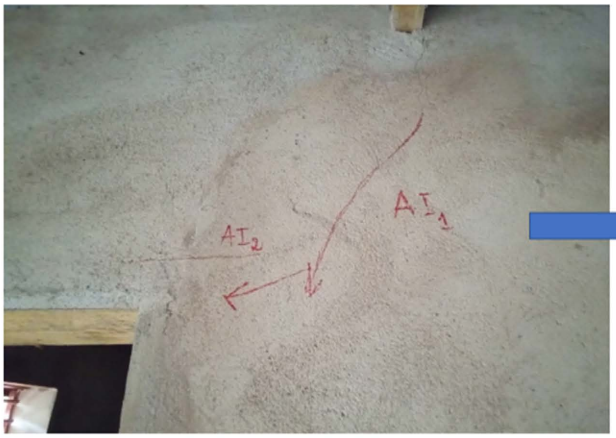

Photo 1: Adobe. Intermediate crack. February 2023 *Richard Z. feb. 2023*

Photo 2: Adobe. Transformation of intermediate cracks into structural crack. June2023 *Richard Z. June 2023*

Photo 7: Exterior view of the breeze-block witness habitat in June 2022. *Richard Z. June 2023*

Photo 8: Exterior view of the breeze-block witness habitat in June 2023. *Richard Z. June 2023*

Photo 9: Exterior view of the cut laterite bricks' witness habitat in June 2022. *Richard Z. June 2022*

Photo 10: Exterior view of the cut laterite bricks' witness habitat in June 2023. *Richard Z. June 2023*

Figure 1. Photographs of the physical degradation of witness houses.

sublevels, filled with cemented rock fill (CRF); 21% longhole retreat using up holes, without backfill, and recovery of sill areas between mining fronts; and 6% crown pillar mining, followed by cut and fill and final uphole retreat. Six mining blocks are planned to ensure sufficient independent mining fronts. For more

details, refer to Figure 3 & Figure 4. Ore development along the vein is limited to a maximum width of 5 m. Blast holes consist of parallel down holes 14 to 16 m in length, loaded with either ammonium nitrate-fuel oil (ANFO) or emulsion, depending on local water conditions, at an average powder factor of 0.5 kilograms per ton.

2.2. Peak Particle Velocity (PPV) Monitoring

Seismic wave monitoring equipment includes seismographs, vibrometers, and

Figure 2. Aerial view of the Yaramoko gold mine area with surface infrastructure (source: AUMS, 2022).

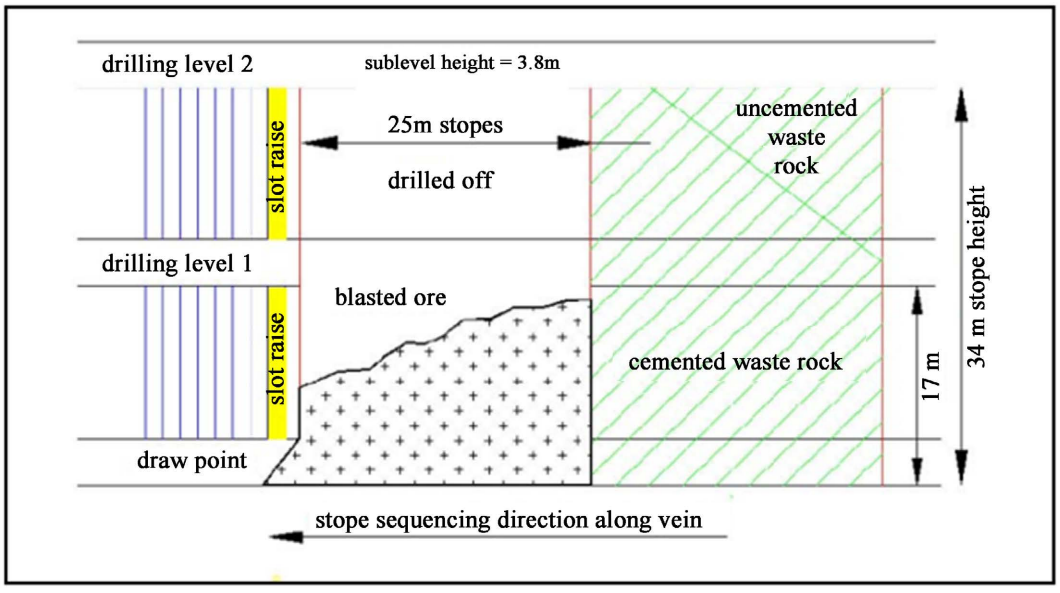

Figure 3. Typical long section—long hole open stope [6].

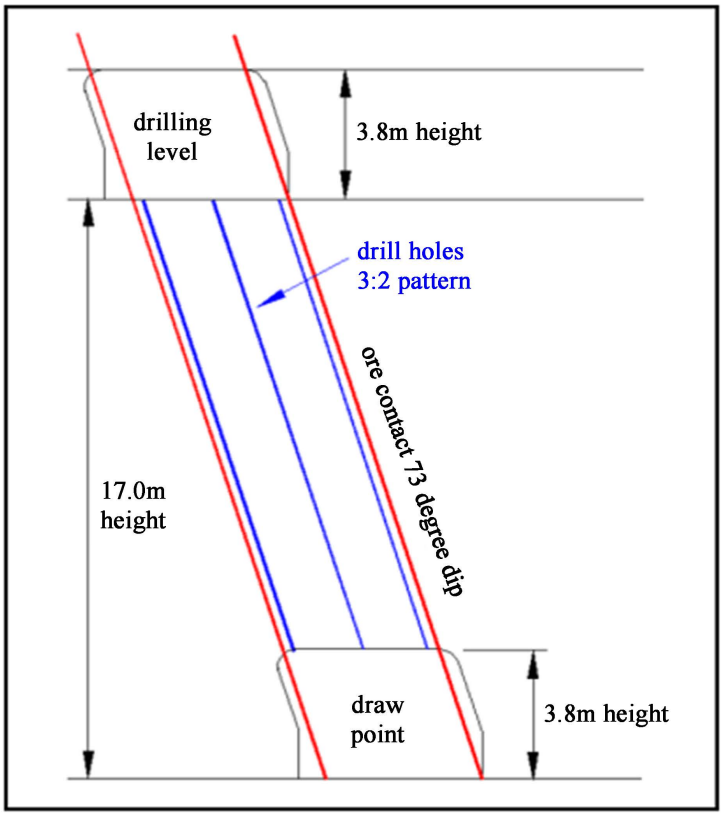

Figure 4. Cross-section—long hole open stope typical sublevel, 4.0 m width [6].

accelerometers. In our study, four seismographs were used: two Instantel Micromate ISEE (std/IO) devices, one Vibrock V901 device, and one Svantek 977 device. A Cirrus integrated sound level meter (CR:821C) was employed for noise level measurements, and a Davis 6152 Wireless Vantage Pro2 Weather Station was used to collect climate data for the site. The geolocations for the study were determined using a GPS GARMIN 64 S. Distance measurements were made with a caliper (to measure wall spacing during a crack), an infrared rangefinder, and a tailor's tape measure. The vibration measurement points and the blasting area were situated at the same elevation. The distances between the measurement points and the blasting area were calculated using the Pythagorean theorem, as shown in **Figure 5**.

2.3. PPV Predicting Equations

Numerous research studies have proposed several empirical equations to describe the attenuation characteristics of blast vibrations and predict the attenuation of Peak Particle Velocity (PPV). In most of these equations, the radial distance and the charge weight per delay are considered the primary parameters influencing PPV prediction. However, it is well known that PPV is also affected by other factors, such as rock strength, rock mass discontinuities, and blast geometry, which have not been explicitly incorporated into these empirical equations. Recent studies have analyzed vibration data across multiple case studies, differing in terms of

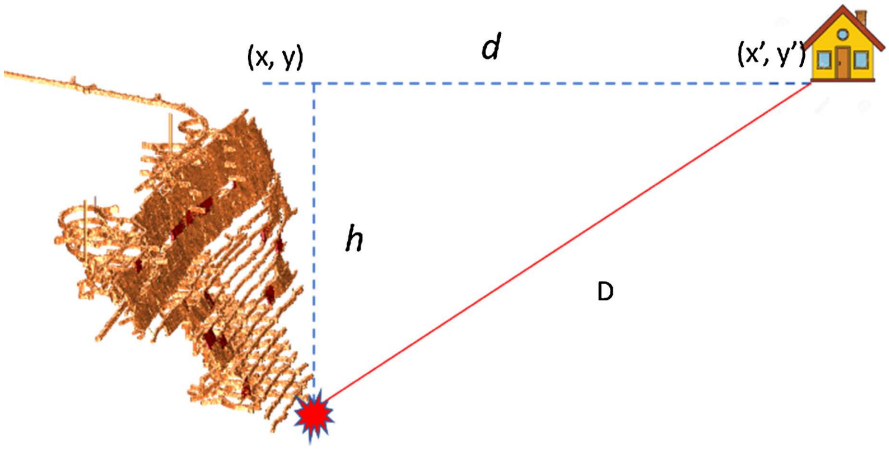

Figure 5. Schematic illustration of blasting position and PPV measurement points. Note that D represents the radial distance from the blasting center to the vibration measurement point.

both operations and rock types [7] [8]. In the present study, four empirical equations are used as the prediction models: Duvall & Fogelson [9], Langefors and Kihlstrom [10], Ambressys-Hendron [11], and the Bureau of Indian Standard [12]. These equations are summarized in **Table 1**. Note that the parameter D represents the radial distance from the blasting center to the vibration measurement point (**Figure 5**). The parameter Q refers to the charge weight used for the initial detonation. The parameters k and n, known as site constants, are positive coefficients determined empirically through linear regression and are dependent on local blasting conditions.

Table 1. Empirical PPV prediction equations according to different studies. The parameters k and n are dimensionless; *PPV is in mm/s*, *D is in meters*, and *Q is in kilograms*.

Author(s)	Equation
Duvall & Fogelson [9]	$\mathrm{PPV} = k\left(\frac{D}{Q^{\frac{1}{2}}}\right)^{-n}$
Langefors and Kihlstrom [10]	$\mathrm{PPV} = k\left(\frac{D^{\frac{2}{3}}}{Q^{\frac{1}{2}}}\right)^{-n}$
Ambressys-Hendron [11]	$\mathrm{PPV} = k\left(\frac{D^{\frac{1}{3}}}{Q}\right)^{-n}$
Bureau of Indian Standard [12]	$\mathrm{PPV} = k\left(\frac{D}{Q^{\frac{2}{3}}}\right)^{-n}$

The four empirical PPV prediction equations lead to a general relation of the form [13]:

$$\text{PPV} = k\left(\frac{D^{\alpha}}{Q^{\beta}}\right)^{-n}$$

The two parameters, k and n, need to be determined to obtain the PPV prediction equation as a function of a scaled distance factor, $\left(\frac{D^{\alpha}}{Q^{\beta}}\right)$.

Based on the measurement data, the parameters k and n are obtained by plotting a linear regression equation:

$$\log_{10}\text{PPV} = f\left(\log_{10}\left(\frac{D^{\alpha}}{Q^{\beta}}\right)\right) = -n\log_{10}\left(\frac{D^{\alpha}}{Q^{\beta}}\right) + \log_{10} k = -ax + b$$

where $n = a$ and $\log_{10} k = b$.

2.4. Monitoring Physical Degradation

In theory, all infrastructure has a lifespan beyond which signs of deterioration begin to appear. The construction materials used, along with the climatic conditions and various pressures the infrastructure is subjected to, negatively impact its lifespan. In general, for all types of materials, the appearance and progression of both intermediate and structural cracks can be observed. Almost all intermediate cracks are the origin of structural cracks, which extend and worsen over time. Figure 6 illustrates the theoretical behavior of crack development over time in infrastructures, whether subjected to external shocks or not. In the absence of external disturbances, the number of cracks increases almost linearly over time (Figure 6(a)). However, in the presence of external disturbances, a sudden increase in the number of cracks is observed (Figure 6(b)) because of the increase in stress concentration. [13]

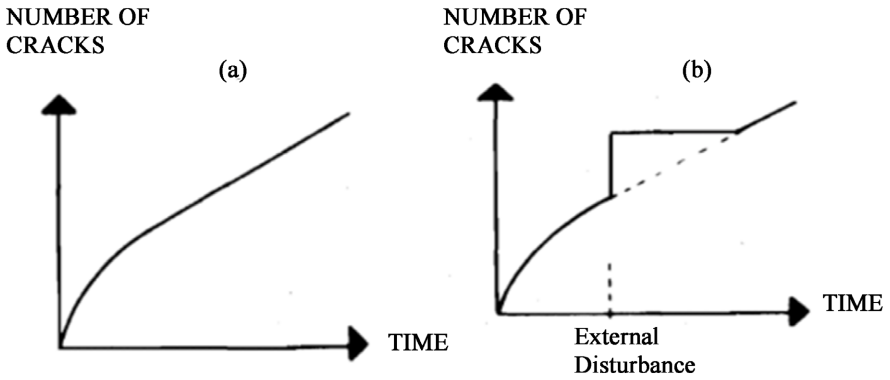

Figure 6. Crack development over time in infrastructures: (a) not subject to external shocks; (b) subject to external shocks [14].

In the present study, the infrastructures used to assess physical degradation due to blasting vibrations can be classified into two categories. The first category, referred to as "witness houses," consists of new houses constructed specifically for the study. Their materials and dimensions were determined based on a study conducted in 2021 on existing houses located within a radius of approximately 2 km

from the mine. Three types of witness houses were considered: cinder block, laterite block, and banco bricks. The second category of infrastructure comprises the residential houses of the local population. A total of 213 houses, spread across five villages near the mine, were included in the study: 55 cinder block houses (25.82%), 80 laterite block houses (37.55%), and 78 banco brick houses (36.61%).

3. Results

3.1. PPV Predicting Equations

Table 2 presents the blasting measurement data collected between June and October 2022. According to several studies [15] [16], the maximum value of the

Table 2. Blasting measurement data collected between June and October 2022 for the study of the PPV predicting equation. Trans.: Transversal; Vert.: Vertical; Long.: Longitudinal; Max.: Maximum.

N°	Date	PPV (mm/s)				Charge (kg)	Radiale distance D(m)
		Trans.	Vert.	Long.	Max.		
1	8-Jun-22	1.789	0.922	1.734	1.789	34.90	544
2	8-Jun-22	1.119	1.056	1.23	1.23	27.60	544
3	9-Jun-22	1.986	0.883	1.986	1.986	41.2	643
4	13-Jun-22	0.883	0.528	1.08	1.08	43.3	778
5	21-Jun-22	1.474	0.883	1.395	1.474	23.2	461
6	24-Jun-22	1.237	0.828	1.19	1.237	33.6	721
7	27-Jun-22	2.877	1.655	2.246	2.877	30.9	452
8	5-Jul-22	1.143	0.67	1.017	1.143	36.8	666
9	8-Jul-22	1.23	0.875	1.088	1.23	44.8	775
10	9-Jul-22	1.111	0.709	0.938	1.111	49.9	885
11	12-Jul-22	1.277	0.804	0.843	1.277	51.6	886
12	14-Jul-22	1.427	0.954	0.906	1.427	40.20	664
13	15-Jul-22	1.687	0.899	0.985	1.687	40.1	664
14	15-Jul-22	1.513	0.757	0.922	1.513	39.7	664
15	18-Jul-22	1.064	0.599	1.159	1.159	52	886
16	21-Jul-22	0.962	0.465	1.001	1.001	53	885
17	22-Jul-22	1.151	0.552	1.072	1.151	52	885
18	7-Aug-22	1.813	1.198	1.324	1.813	30.50	434
19	2-Sep-22	3.76	1.521	1.671	3.76	32.30	451
20	14-Sep-22	2.79	1.758	3.318	3.318	32.40	419
21	28-Oct-22	2.885	1.135	2.16	2.885	30.00	433
22	30-Oct-22	1.198	0.552	1.009	1.198	29.90	434

transverse, vertical, and longitudinal components of the measured PPV is used to predict the PPV equation.

Figure 7 shows the linear regression curves based on the four PPV equations. The coefficient of determination (R^2) ranges from 0.60 to 0.68, which is comparable to values reported in similar studies [15] [17]-[20]. The site constants k and n, deduced from the linear regression equations, are provided in Table 3. For the Duvall & Fogelson equation, also known as the USBM equation or Chapot's law, the n value of 1.74 is slightly lower than the theoretical value of 1.8. For the Ambraseys-Hendron equation, also known as the surface wave law, the *n* value of 1.44 is higher than the theoretical value of 1.2.

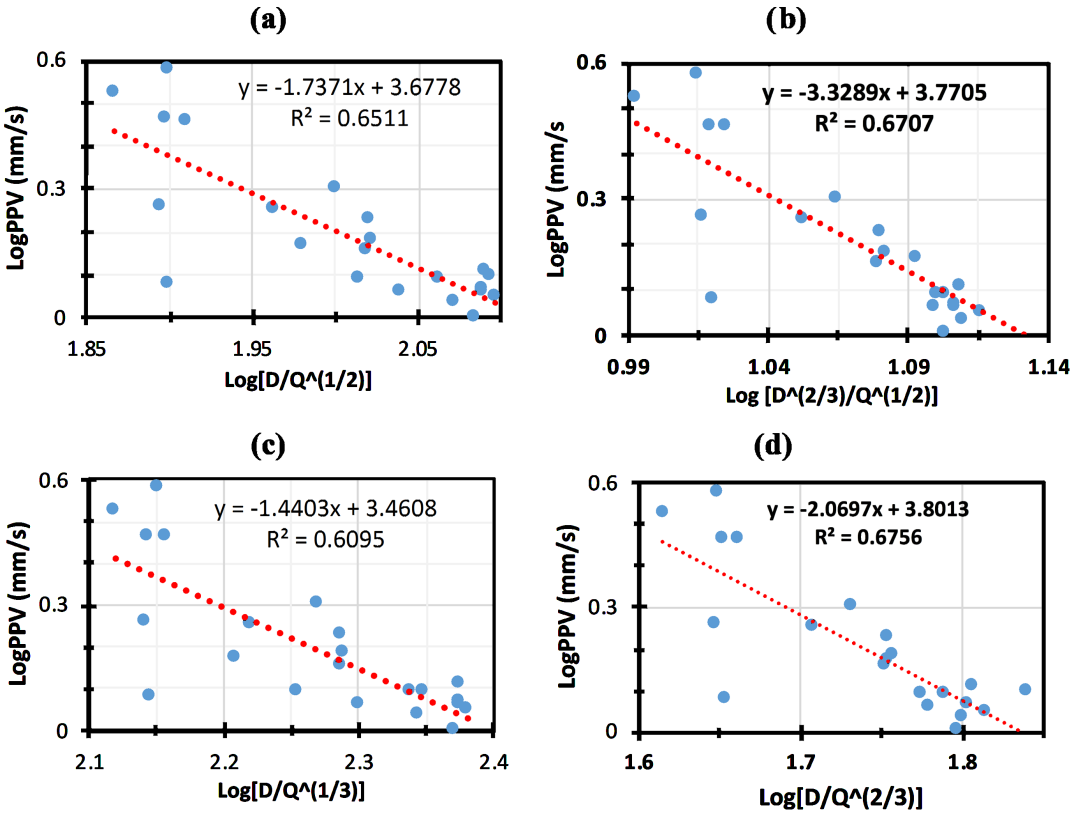

Figure 7. Logarithmic plot of Peak Particle Velocity (PPV) as a function of scaled distances $\left(\frac{D^{\alpha}}{Q^{\beta}}\right)$. (a) Duvall & Fogelson [9]; (b) Langefors and Kihlstrom [10]; (c) Ambraseys and Hendron [11]; (d) Bureau of Indian Standards [12].

Table 4 presents recent comparative results of PPV predicting equations based on the general PPV prediction equation by Davies [21]-[23]:

$$\mathrm{PPV} = kQ^{a}D^{-b}$$

Given that the geological study of the Yaramoko mine is dominated by granitoid, including quartz rocks [6], the site constants *k*, *a*, and *b* of 4762, 0.869, and 1.737, respectively deduced from the Duvall & Fogelson equation in the present study align closely with the values of 4690, 0.9, and 1.69 for similar rock types in

Table 3. Summary of constants by type of equation.

Equation	k	n	R^2	Reference
$\mathrm{PPV} = k\left(\frac{D}{Q^{\frac{1}{2}}}\right)^{-n}$	4762	1.7371	0.651	[9]
$\mathrm{PPV} = k\left(\frac{D}{Q^{\frac{1}{3}}}\right)^{-n}$	2889	1.4403	0.609	[11]
$\mathrm{PPV} = k\left(\frac{D^{\frac{2}{3}}}{Q^{\frac{1}{2}}}\right)^{-n}$	2232	3.3289	0.671	[10]
$\mathrm{PPV} = k\left(\frac{D}{Q^{\frac{2}{3}}}\right)^{-n}$	6328	2.0697	0.676	[12]

Table 4. Comparative results of PPV equations.

Reference	Equation	R^2
Present work	$\mathrm{PPV} = 4762Q^{0.869}D^{-1.737}$	0.651
	$\mathrm{PPV} = 2889Q^{0.8}D^{-1.44}$	0.609
	$\mathrm{PPV} = 2232Q^{1664}D^{-2.219}$	0.671
	$\mathrm{PPV} = 6328Q^{1.38}D^{-2.07}$	0.676
Rodriguez *et al.* [8]	$\mathrm{PPV} = 4690Q^{0.9}D^{-1.69}$	0.883
Hammed *et al.* [24]	$\mathrm{PPV} = 3467Q^{0.595}D^{-1.19}$	1.0
	$\mathrm{PPV} = 3631Q^{0.73}D^{-1.46}$	
	$\mathrm{PPV} = 3631Q^{0.69}D^{-1.38}$	
	$\mathrm{PPV} = 6310Q^{0.865}D^{-1.73}$	
	$\mathrm{PPV} = 4169Q^{0.8}D^{-1.6}$	

Spain [8]. In the work by Hammed *et al.* [24], conducted at quarry sites in Nigeria, the equations in Table 4 derived from the Duvall & Fogelson PPV prediction model were deduced from data in a logarithmic plot of Peak Particle Velocity against scaled distance datasets. Although the specific rock types at the quarry sites were not mentioned, the equation with site constants k, a, and b of 4169, 0.8, and 1.6, respectively, are consistent with the values noted above. As the values of the site constants reflect both the quality of the shot and the transmission of vibrations through the rock mass, we conclude that these factors explain the differences between the present results and those obtained in Spain.

3.2. Damage Tracking

Figure 8 presents the results showing the average number of cracks per type of

construction material, primarily influenced by blasting impacts. Degradation data were collected over a 12-month period (June 2022 to June 2023) from 213 residential houses and three (3) witness houses, as previously mentioned in section 2.4. The degradation criteria were established with the assistance of an approved architectural firm in Burkina Faso. A total of four visits were made to the residential houses to assess any physical degradation, while the three witness houses were monitored daily.

Comparing the evolution of the curves in Figure 8 with those in Figure 6, along with their descriptions, it becomes evident that blasting vibrations significantly affect the physical integrity of houses. The extent of degradation depends on the types of materials used for construction. In the context of the Bagassi area, and based on the characteristics of the curves in Figure 8(b), houses constructed with laterite blocks are the most vulnerable to blasting vibrations, followed by houses made from cinder blocks. In contrast, houses made from banco are more resistant, although this material is more susceptible to weather conditions.

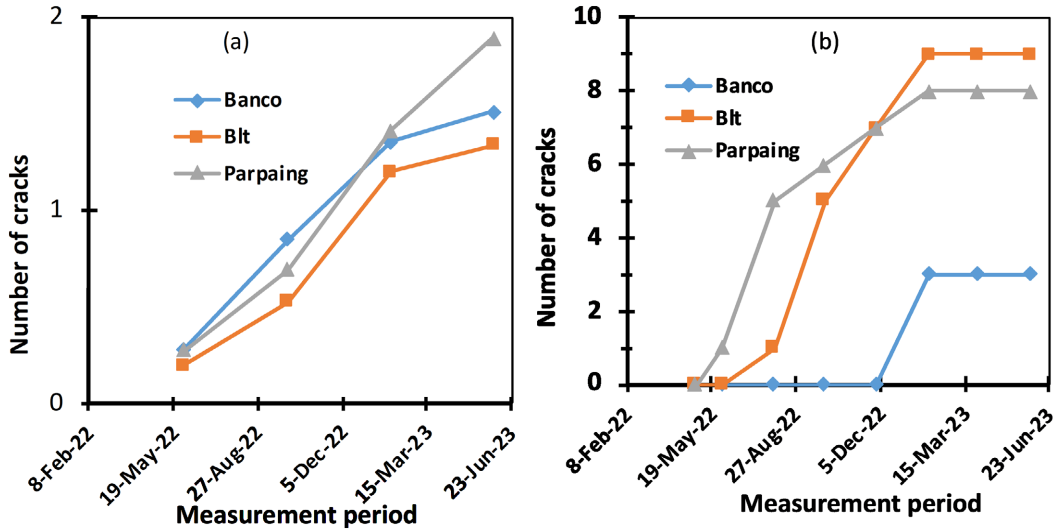

Figure 8. Average number of cracks per material type: (a) residential houses; (b) witness houses.

The differences in the curve evolution for residential houses (Figure 8(a)) compared to witness houses (Figure 8(b)) can mainly be attributed to the intensity of blasting vibrations experienced by each. The residential houses, which are of the same type as the witness houses of type F2, are all located within a 2 km radius of the mine site and are therefore subject to the same climatic conditions. However, since the witness houses are situated inside the mine site, they are more exposed to blasting vibrations compared to the residential houses located outside the mine. The lower number of cracks in the residential houses (Figure 8(a)) compared to the higher number in the witness houses (Figure 8(b)) can be explained by the fact that residential houses are exposed to fewer external factors apart from climatic conditions, which can be considered normal for the region. Meanwhile, the witness houses, in addition to climatic hazards, are subjected to external shocks of

vibrations from the blasting operations conducted as part of the mining activities.

In terms of the age of the buildings, the witness houses were newer than the residential ones, which were between 1 and 3 years old. Consequently, at the start of the monitoring period, the residential houses were already showing cracks, whereas the witness houses could be considered in the initial stages of degradation. The higher number of cracks observed in the witness houses one year later, compared to the residential houses, provides evidence of the effects of blasting vibrations on buildings.

The above results regarding the physical degradation of houses due to blasting vibrations are consistent with the compressive strength analyses carried out on the three types of bricks (laterite block, cinder block, and banco) used for construction. The results revealed that the most resistant of the three types of bricks is banco, with 75% of the analyzed samples having a compressive strength higher than 3.2 MPa, which is the minimum required compressive strength for building bricks (class 40) according to standard NFP 14-301. The least resistant bricks are laterite blocks, which are extracted locally from a quarry in the village of Bagassi. Their calculated compressive strength ranges from 0.8 to 1.8 MPa, with an average of 1.3 MPa. As for the cinder blocks, they exhibit an average compressive strength of 1.9 MPa. Neither the laterite block bricks nor the cinder block bricks meet the minimum required compressive strength.

3.3. Determination of Blasting Parameters Avoiding Crack

Figure 9 shows the relationship between PPV and the progression of crack formation. The witness houses previously described are used for this study, with construction completed in mid-May 2022. In the case of the cinder-block witness house, the first intermediate crack appeared on June 16, 2022, following a blast

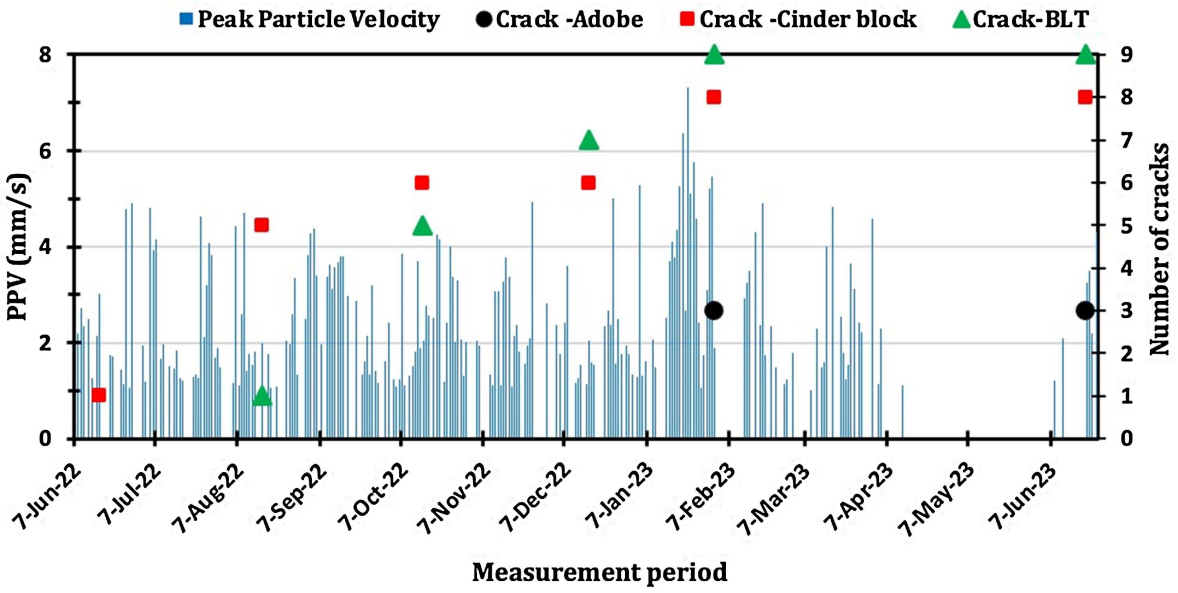

Figure 9. Crack appearance as a function of seismic waves.

with a recorded PPV of 3.02 mm/s. From that point on, the average PPV value was 1.98 mm/s. Over time, the intermediate crack grew in length and severity, leading to the first structural crack in the block by the 8th month of monitoring.

For the laterite block witness house, with 69 blasts exhibiting a PPV greater than 1 mm/s and an average of 2.14 mm/s, the highest PPV recorded before the appearance of a crack was 4.89 mm/s. Similarly, for the banco witness house, with 231 blasts showing a PPV greater than 1 mm/s and an average of 2.30 mm/s, the highest PPV before a crack appeared was 7.31 mm/s. These results indicate three reference PPV values associated with the appearance of the first intermediate crack in the witness houses: 3.02 mm/s for the cinder-block house, 4.89 mm/s for the laterite block house, and 7.31 mm/s for the banco house. The average PPV values during the blasts were 1.98 mm/s, 2.14 mm/s, and 2.3 mm/s, respectively.

Based on these findings, it can be concluded that a PPV of 2 mm/s or less for dwellings near mines, resulting from vibrations caused by blasting, would minimize the likelihood of cracks in the buildings. This conclusion aligns with the requirements of the Republic of Ghana's standard, which limits the PPV to no more than 2 mm/s at the level of neighboring communities to ensure their physical and social safety during blasting operations [25].

To determine the blasting parameters, specifically the charge (Q) and the vertical distance from the blasting center to its projection on the ground (h) (see **Figure 5**), that respect the threshold value of 2 mm/s for a given horizontal distance, d, representing the location of the houses) (see **Figure 5**), the values of the PPV prediction equation as a function of the charge (Q) and the vertical distance (h) are presented in **Table 5** & **Table 6**. The shaded cells correspond to the values of

Table 5. Estimated values of $\mathrm{PPV} = kQ^a D^{-b}$ with $D = \sqrt{d^2 + h^2}$ as a function of charge (Q) and blasting vertical distance (h) for the values of $k = 4762$, $a = 0.869$, $b = 1.737$, and $d = 220$ m.

h (m)	Q (kg)						
	10	20	30	40	50	60	70
300	1.21	2.20	3.14	4.03	4.89	5.73	6.55
325	1.10	2.01	2.86	3.67	4.45	5.22	5.97
350	1.00	1.84	2.61	3.35	4.07	4.77	5.45
375	0.92	1.68	2.39	3.07	3.73	4.37	4.99
400	0.85	1.54	2.20	2.82	3.43	4.01	4.59
425	0.78	1.42	2.02	2.60	3.16	3.70	4.23
450	0.72	1.31	1.87	2.40	2.92	3.42	3.91
475	0.67	1.22	1.73	2.22	2.70	3.16	3.62
500	0.62	1.13	1.61	2.07	2.51	2.94	3.36
525	0.58	1.05	1.50	1.92	2.33	2.74	3.13

Continued

550	0.54	0.98	1.40	1.79	2.18	2.55	2.92
575	0.50	0.92	1.31	1.68	2.04	2.39	2.73
600	0.47	0.86	1.23	1.57	1.91	2.24	2.56
625	0.44	0.81	1.15	1.48	1.79	2.10	2.40
650	0.42	0.76	1.08	1.39	1.69	1.98	2.26
675	0.39	0.72	1.02	1.31	1.59	1.86	2.13
700	0.37	0.68	0.96	1.24	1.50	1.76	2.01
725	0.35	0.64	0.91	1.17	1.42	1.66	1.90
750	0.33	0.61	0.86	1.11	1.35	1.58	1.80
775	0.32	0.58	0.82	1.05	1.28	1.50	1.71
800	0.30	0.55	0.78	1.00	1.21	1.42	1.63
825	0.29	0.52	0.74	0.95	1.15	1.35	1.55
850	0.27	0.50	0.71	0.91	1.10	1.29	1.47

Table 6. Estimated values of $\mathrm{PPV} = kQ^{a}D^{-b}$ with $D = \sqrt{d^2 + h^2}$ as a function of charge (Q) and blasting vertical distance (h) for the values of $k = 4762$, $a = 0.869$, $b = 1.737$ and $d = 500$ m.

h (m)	Q (kg)						
	10	**20**	**30**	**40**	**50**	**60**	**70**
200	0.63	1.16	1.65	2.12	2.57	3.01	3.44
225	0.62	1.12	1.60	2.05	2.49	2.92	3.34
250	0.59	1.09	1.55	1.98	2.41	2.82	3.23
300	0.55	1.01	1.44	1.84	2.24	2.62	3.00
325	0.53	0.97	1.38	1.77	2.15	2.52	2.88
350	0.51	0.93	1.33	1.70	2.07	2.42	2.77
375	0.49	0.90	1.27	1.64	1.98	2.33	2.66
400	0.47	0.86	1.22	1.57	1.90	2.23	2.55
425	0.45	0.82	1.17	1.50	1.82	2.14	2.44
450	0.43	0.79	1.12	1.44	1.75	2.05	2.34
475	0.41	0.75	1.07	1.38	1.67	1.96	2.24
500	0.40	0.72	1.03	1.32	1.60	1.88	2.15
525	0.38	0.69	0.98	1.26	1.53	1.80	2.05
550	0.36	0.66	0.94	1.21	1.47	1.72	1.97
575	0.35	0.63	0.90	1.16	1.41	1.65	1.88
600	0.33	0.61	0.86	1.11	1.35	1.58	1.81

Q and h that result in PPV values greater than 2 mm/s. Using this data, it becomes possible to conduct blasting operations with minimal impact on nearby homes. For example, for a charge weight between 40 and 60 kg, vertical distances (h) of more than 600 m and 500 m are recommended when the houses are located 220 m (the distance of the witness houses in this study) and 500 m (the standard distance to maintain in Burkina Faso), respectively.

4. Conclusion

The aim of this study was to determine the site constants in order to define the experimental law of Peak Particle Velocity (PPV) related to the propagation of vibrations caused by rock blasting at the Yaramoko mine. Additionally, it sought to identify the maximum PPV value that minimizes the impact of vibrations on houses near the mine. Based on previous research, various empirical PPV prediction equations were established, which could also be applied to mining sites with a predominance of granitoid rocks, as is the case for mines in Burkina Faso. It has also been established that during blasting operations, it is possible to minimize the appearance of cracks in nearby buildings by adjusting the blasting parameters to ensure that the PPV does not exceed 2 mm/s. This study was conducted in an underground mine setting. Expanding this research to other similar mines and open-pit mines will help consolidate data related to predicting particle velocity induced by blasting in the context of Burkina Faso.

Acknowledgements

The authors are grateful to Roxgold Sanu Mining Company for allowing this research to be conducted at its site.

Conflicts of Interest

The authors declare no conflicts of interest regarding the publication of this paper.

References

[1] Ouédraogo, I. (1994) Géologie et hydrogéologie des formations sedimentaires de la Boucle du Mouhoun (Burkina Faso). Ph.D. Thesis, Université Cheikh Anta Diop de Dakar. https://beep.ird.fr/collect/uouaga/index/assoc/M07215.dir/M07215.pdf

[2] Bureau Voltaique de la Géologie et des Mines (1984) Note sur les possibilités d'existence d'hydrocarbures et d'autres substances energetiques au Burkina Faso et propositions pour leur prospection. https://inis.iaea.org/collection/NCLCollectionStore/_Public/39/061/39061810.pdf

[3] Synduex (2018) Guide d'utilisation des explosifs en travaux publics.

[4] Rawnaq, E., Esmatyar, B., Hamanaka, A., Sasaoka, T. and Shimada, H. (2024) A Comparative Study of Two Tree-Based Models for Predicting Flyrock Velocity at Open Pit Bench Mining. *Open Journal of Applied Sciences*, **14**, 267-287. https://doi.org/10.4236/ojapps.2024.142019

[5] Guth, K., Bourgeois, M. and Harbison, R. (2022) Assessment of Lead Exposures during Abrasive Blasting and Vacuuming in Ventilated Field Containments: A Case

Study. *Occupational Diseases and Environmental Medicine*, **10**, 116-131. https://doi.org/10.4236/odem.2022.102010

[6] SRK Consulting (2014) Technical Report for the Yaramoko Gold Mine, Burkina Faso. Roxgold Inc.

[7] Cardu, M., Coragliotto, D. and Oreste, P. (2019) Analysis of Predictor Equations for Determining the Blast-Induced Vibration in Rock Blasting. *International Journal of Mining Science and Technology*, **29**, 905-915. https://doi.org/10.1016/j.ijmst.2019.02.009

[8] Rodríguez, R., García de Marina, L., Bascompta, M. and Lombardía, C. (2021) Determination of the Ground Vibration Attenuation Law from a Single Blast: A Particular Case of Trench Blasting. *Journal of Rock Mechanics and Geotechnical Engineering*, **13**, 1182-1192. https://doi.org/10.1016/j.jrmge.2021.03.016

[9] Duvall, W.I. and Fogelson, D.E. (1962) Review of Criteria for Estimating Damage to Residences from Blasting Vibrations. https://api.semanticscholar.org/CorpusID:107939815

[10] Langefors, U. and Kihlström, B. (1978) The Modern Technique of Rock Blasting. Wiley.

[11] Ambraseys, N.N. and Hendron, A.J. (1968) Dynamic Behaviour of Rock Masses. John Wiley & Sons.

[12] Bureau of Indian Standards (1973) Criteria for Safety and Design of Structures Subject to Underground Blasts. https://dn790004.ca.archive.org/0/items/gov.in.is.6922.1973/is.6922.1973.pdf

[13] Ongen, T., Karakus, D., Konak, G. and Onur, A.H. (2018) Assessment of Blast-Induced Vibration Using Various Estimation Models. *Journal of African Earth Sciences*, **145**, 267-273. https://doi.org/10.1016/j.jafrearsci.2018.05.004

[14] Holmberg, R., Lundborg, N. and Rundqvist, G. (1983) Soil Vibrations and Damage Criteria. National Research Council of Canada. https://doi.org/10.4224/20358507

[15] Giraudi, (2009) An Assessment of Blasting Vibrations: A Case Study on Quarry Operation. *American Journal of Environmental Sciences*, **5**, 468-474. https://doi.org/10.3844/ajessp.2009.468.474

[16] Kadiri, I., Tahir, Y., Iken, O., Fertahi, S.E.-D. and Agounoun, R. (2019) Experimental and Statistical Analysis of Blast-Induced Ground Vibrations (*BIGV*) Prediction in Senegal's Quarry. *Studia Geotechnica et Mechanica*, **41**, 231-246. https://doi.org/10.2478/sgem-2019-0025

[17] Chapot, P. (1981) Loi expérimentale de propagation des vibrations dues aux tirs d'explosifs. *Revue Française de Géotechnique*, No. 14, 109-113. https://doi.org/10.1051/geotech/198114b109

[18] Kanon Ghislain, A., Ouattara, G. and Anon Felix, N. (2022) Prediction of Vibrations Due to Blast at the Hiré Mine, Côte D'ivoire. *International Journal of Environmental Monitoring and Analysis*, **10**, 32-38. https://doi.org/10.11648/j.ijema.20221002.12

[19] Khandelwal, M., Armaghani, D.J., Faradonbeh, R.S., Yellishetty, M., Majid, M.Z.A. and Monjezi, M. (2016) Classification and Regression Tree Technique in Estimating Peak Particle Velocity Caused by Blasting. *Engineering with Computers*, **33**, 45-53. https://doi.org/10.1007/s00366-016-0455-0

[20] Azimi, Y. (2019) Prediction of Seismic Wave Intensity Generated by Bench Blasting Using Intelligence Committee Machines. *International Journal of Engineering*, **32**, 617-627. https://doi.org/10.5829/ije.2019.32.04a.21

[21] Davies, B., Farmer, I.W. and Attewell, P.B. (1964) Ground Vibration from Shallow

Sub-Surface Blasts. TRID.

[22] Nicholls, H.R., Johnson, C.F and Duvall, W.I. (1971) Blasting Vibrations and Their Effects on Structures. Technical Report, Bureau of Mines, Washington, DC. https://api.semanticscholar.org/CorpusID:106811312

[23] Fouladgar, N., Hasanipanah, M. and Bakhshandeh Amnieh, H. (2016) Application of Cuckoo Search Algorithm to Estimate Peak Particle Velocity in Mine Blasting. *Engineering with Computers*, **33**, 181-189. https://doi.org/10.1007/s00366-016-0463-0

[24] Hammed, O.S., Popoola, O.I., Adetoyinbo, A.A., Awoyemi, M.O., Adagunodo, T.A., Olubosede, O., *et al.* (2018) Peak Particle Velocity Data Acquisition for Monitoring Blast Induced Earthquakes in Quarry Sites. *Data in Brief*, **19**, 398-408. https://doi.org/10.1016/j.dib.2018.04.103

[25] Ghana (2012) Minerals and Mining (Explosives) Regulations, 2012 (Li 2177). Ghana Publishing Company.